Int. J. Heat Mass Transfer. Vol. 32, No. 4, pp. 689–696, 1989
Printed in Great Britain

0017–9310/89 $3.00 + 0.00
© 1989 Pergamon Press plc

Engineering analysis of heat transfer during melting in vertical rectangular enclosures

WOON-SHING YEUNG
Department of Mechanical and Energy Engineering, University of Lowell, Lowell, MA 01854, U.S.A.

(*Received* 1 *June* 1988 *and in final form* 25 *August* 1988)

Abstract—This paper presents a simple engineering analysis method for the heat transfer process during melting in a vertical rectangular enclosure. The analysis is based on the conduction layer approximate method (CLAM) previously applied to study natural convection without phase change in enclosures. Similar to most existing numerical schemes, the present model tracks the melting front during the melting process. However, detailed velocity and temperature fields are not required. Numerical results are generated with relative ease and insignificant computer times. Comparison is made with existing numerical studies and experimental data for the time development of the melting front and the melted fraction. Good agreement is obtained.

INTRODUCTION

ANALYSES of heat transfer during melting of a phase change material (PCM) in rectangular enclosures are complicated due to the presence of natural convection in an irregular, time-dependent melt region. Numerical studies [1–4] usually employ a transformation which maps the irregular time-dependent domain into a fixed rectangular computational domain. The transformed governing equations of motion for the liquid phase are then solved by various numerical means. In general, results from these numerical studies compare adequately with experimental data. However, the reported large computer times of these codes preclude as yet their practical usage in engineering analyses of phase change systems.

In order to significantly reduce computational times, alternative numerical methodologies, such as boundary element techniques [5], finite element methods, and vectorized programming, must be adopted with the mathematical model presently used in the literature. Another approach is to develop new analytical methodologies for systems undergoing a phase change process. To this end, for instance, a simple semi-analytical correlation has been derived for the prediction of the melted fraction of a PCM inside a rectangular enclosure [2]. In ref. [6], a planar approximation of the melting front yields a simple formula for the melted fraction in an inclined enclosure. From experimental measurements of the tube wall temperature during solidification around a tube, the time development of the phase change front has been predicted [7]. Finally, an enthalpy model that takes into account natural convection has been proposed [8, 9], which allows the use of a fixed computational grid in the numerical solution.

This paper presents a simple engineering analysis of the heat transfer process during melting in a vertical rectangular enclosure. The analysis is based on the conduction layer approximate method (CLAM) [10] which has been successfully applied to study the natural convection process inside a vertical rectangular enclosure [11]. The primary quantity of interest in the present study is the time development of the melting front. Neither the two-dimensional velocity field nor the detailed two-dimensional temperature field needs to be evaluated. Numerical results are generated with straightforward programming and insignificant computer times. Comparisons are made with existing numerical and experimental data [2–4] and good agreement is obtained.

PROBLEM DEFINITION AND MODEL ASSUMPTIONS

Figure 1 shows a vertical rectangular enclosure initially containing a PCM at its fusion temperature T_f. Melting is started by raising the temperature of the left wall to T_w ($> T_f$). The top and bottom walls of the enclosure are insulated. Most studies model a free surface on the top of the PCM due to the air gap normally required in experiments. The effects of this air gap are ignored in the present analysis.

At the beginning, the melting process is controlled by conduction through the small melt layer. The corresponding melting front is vertical. As the melt layer increases, natural convection which transports the hotter fluid to the top and the colder fluid to the bottom becomes important. As a result, the amount of heat transfer to the melting front increases with the vertical distance from the bottom of the enclosure. The melting front is no longer vertical but takes on the typical shape depicted in Fig. 1. The subsequent development of the melting front is controlled by natural convection of the liquid bounded by the melting front itself and part of the enclosure walls.

NOMENCLATURE

A	aspect ratio, H/L
C	coefficient defined by equation (2)
c_p	specific heat
F	function defined by equation (4)
Fo	Fourier number, $\alpha t/L^2$
g	gravity
g_x	gravity in the x-direction
H	height of enclosure
h	heat transfer coefficient
Δh_f	latent heat
K	conductivity
L	length of enclosure
l	characteristic length
Nu_l	Nusselt number, hl/K
n	empirical coefficient, normal coordinate
Pr	Prandtl number
q''	heat flux
Ra_l	Rayleigh number, $g\beta\Delta Tl^3/\nu\alpha$
Ra_L	Rayleigh number, $g\beta(T_w-T_f)L^3/\nu\alpha$
S	coefficient in equation (5)
Ste	Stefan number, $c_p(T_w-T_f)/\Delta h_f$
T_i	liquid core temperature
T_f	fusion temperature
T_w	hot wall temperature
t	time
v_n'	normal velocity of melting front
x	surface coordinate.

Greek symbols

α	diffusivity
β	coefficient of expansion
Γ	mass flow rate
δ	melt layer thickness
$\bar{\delta}$	non-dimensional melt layer thickness, δ/L
ζ	non-dimensional coordinate, x/H
θ	dimensionless temperature, $(T_i-T_f)/(T_w-T_f)$
λ	melted fraction
ν	kinematic viscosity
ρ	density
τ	non-dimensional time, $(Ste\,\alpha t)/L^2$
$\bar{\tau}$	non-dimensional time, $(Ste\,\alpha t)/H^2$
ϕ	angle of inclination.

Subscripts

c	cold wall, conduction regime
h	hot wall
k	kth node, or step.

Superscripts

n	old value
$n+1$	new value.

The usual assumptions of laminar, two-dimensional, Newtonian, and incompressible flow in the liquid region are made. Volume change due to melting is neglected. In addition, the melting process is assumed quasi-steady [2, 3]. Thus, the melting process is approximated by a series of steady solutions in a time varying domain the boundaries of which are determined from the previous steady solution.

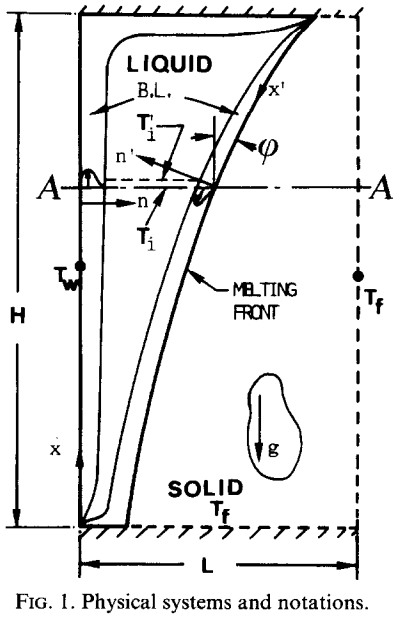

FIG. 1. Physical systems and notations.

CONDUCTION LAYER APPROXIMATE METHOD (CLAM) [7]

Before proceeding to the present model development, a brief description of CLAM is given here. Consider natural convection without phase change in a rectangular enclosure with a temperature difference (T_w-T_f) maintained between the vertical walls, as shown in Fig. 2. There exists a laminar boundary layer (B.L.) regime in which individual boundary layers develop on each vertical wall. The liquid circulation takes place mainly inside these boundary layers. The core, which is the region outside the boundary layers, is nearly stationary. The temperature in the core, T_i, is almost isothermal in the horizontal direction but increases from about T_f at the bottom to about T_w at the top. This thermal stratification in the core is an essential feature of natural convection in vertical enclosures and is largely responsible for the non-uniform movement of the melting front.

In this laminar boundary layer regime, the local Nusselt number is correlated as

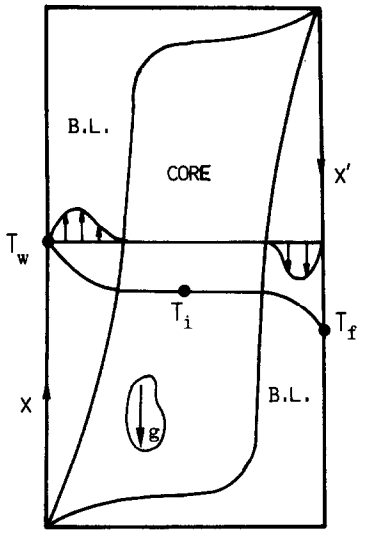

FIG. 2. Notations of CLAM model [7].

$$Nu_l = C\,Ra_l^{0.25}\,F \tag{1}$$

where

$$C = \frac{0.503}{[1+(0.492/Pr)^{9/16}]^{4/9}} \tag{2}$$

$$Nu_l = q''l/K\Delta T, \quad Ra_l = g\beta\Delta T l^3/\nu\alpha \tag{3}$$

$$F = \left\{\frac{\cos^{4/3}\phi\,\Delta T^{1/3-4n/3}}{\frac{1}{l}\int_0^x \cos^{1/3}\phi\,\Delta T^{1/3-4n/3}\,\mathrm{d}x}\right\}^{1/4}. \tag{4}$$

In the above, q'' is the heat flux, ϕ the local angle of inclination of the enclosure wall (which is zero everywhere for a vertical enclosure but will be a function of x when applied to the melt region in the next section), l a characteristic length, ΔT the local temperature difference given by $(T_w - T_i)$ for the hot wall, and $(T_i - T_f)$ for the cold wall, and n an empirical coefficient depending on the Prandtl number. The coordinate x is measured from the leading edge of the surface, which is at the bottom for the hot wall and at the top for the cold wall.

In order to evaluate the Nusselt number and hence the heat flux, the core temperature distribution must be calculated. In CLAM, this is accomplished by applying the principle of mass conservation. It can be shown that the mass flow rate along either wall can be expressed as [11]

$$\Gamma^{4/3} = S\left\{\int_0^x g_x^{1/3}\Delta T^{1/3-4n/3}\,\mathrm{d}x\right\}\Delta T^{4n/3} \tag{5}$$

where the coefficient S contains various ratios appearing in the CLAM model as well as properties of the fluid. In the present analysis, S is assumed constant. By imposing mass conservation at any location x of the enclosure (i.e. the net mass flow rate at any x plane vanishes), the following implicit equation for the core temperature T_i can be derived [11]:

$$\left(\frac{T_i - T_f}{T_w - T_i}\right)^{4n/3} = \frac{\int_0^x (T_w - T_i)^{1/3-4n/3}\,\mathrm{d}x}{\int_x^H (T_i - T_f)^{1/3-4n/3}\,\mathrm{d}x}. \tag{6}$$

Equations (1)–(6) form the theoretical basis for the present study. Their application to the case of melting follows.

MODEL DEVELOPMENT

In melting systems, natural convection takes place in a vertical enclosure having one stationary vertical wall and one moving tilted wall, as again shown in Fig. 1. Under the quasi-steady assumption, the melting front is taken to be stationary while calculations are made of the liquid region. Consider then the horizontal plane A–A. From equation (5), the mass flow rate along the hot wall across A–A is

$$\Gamma_h^{4/3} = S\left\{\int_0^x g^{1/3}(T_w - T_i)^{1/3-4n/3}\,\mathrm{d}x\right\}(T_w - T_i)^{4n/3}. \tag{7}$$

For the cold wall, equation (5) needs to be modified to take account of the tilt. In CLAM, all equations are developed with respect to the surface coordinates. Thus, a transformation from (x', n') to (x, n) must be made to obtain the velocity distribution along A–A at the cold wall. In general, this will be a tedious procedure. To simplify the analysis, therefore, it is assumed that the cold wall velocity distribution along A–A is the same as that written in the original surface coordinates. Thus, the mass flow rate along the cold wall across A–A is given by

$$\Gamma_c^{4/3} = S\left\{\int_0^{x'} g^{1/3}\cos^{1/3}\phi(T_i - T_f)^{1/3-4n/3}\,\mathrm{d}x'\right\} \times (T_i - T_f)^{4n/3}. \tag{8}$$

The factor $\cos^{1/3}\phi$ accounts for the fact that the gravity vector makes an angle ϕ with the area vector of plane A–A. Conservation of mass across A–A then gives

$$\left(\frac{T_i - T_f}{T_w - T_i}\right)^{4n/3} = \frac{\int_0^x (T_w - T_i)^{1/3-4n/3}\,\mathrm{d}x}{\int_x^H (T_i - T_f)^{1/3-4n/3}\cos^{-2/3}\phi\,\mathrm{d}x} \tag{9a}$$

where the following transformation has been used:

$$\mathrm{d}x' = -\mathrm{d}x/\cos\phi. \tag{9b}$$

Equation (9a) can be solved by simple iterative methods to give the core temperature distribution in the vertical direction at any instant.

Having obtained the core temperature distribution, the melting front can be advanced as follows. With

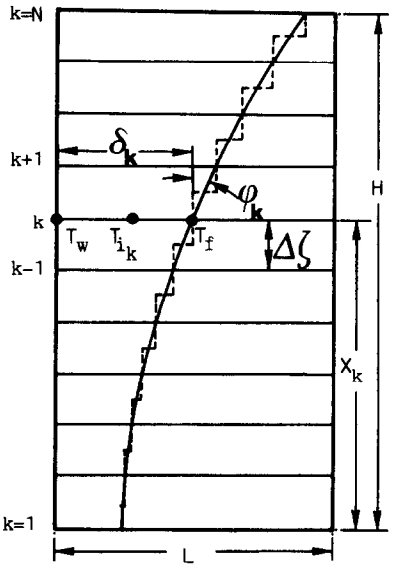

FIG. 3. One-dimensional approximation of melting front.

reference to Fig. 1, the local energy balance at the melting front can be expressed as

$$q'' = h(T_i' - T_f) = \rho \Delta h_f v_n' \tag{10}$$

where v_n' is the local normal velocity of the melting front, and h is the local heat transfer coefficient obtained from equation (1). Equation (10) is rather difficult to use because the unit normal n' is a function of position and time. For simplicity, the melting front is approximated by a series of steps as shown in Fig. 3. A local one-dimensional approximation, which neglects the curvature of the interface, of equation (10) is written for each step as

$$h_k(T_{i_k} - T_f) = \rho \Delta h_f \, \mathrm{d}\delta_k/\mathrm{d}t \tag{11}$$

where the subscript k denotes the kth step at a distance x_k from the bottom wall. In terms of the Nusselt number, one has

$$Nu_k \, K(T_{i_k} - T_f)/l = \rho \Delta h_f \, \mathrm{d}\delta_k/\mathrm{d}t. \tag{12}$$

Equation (12) can be integrated to give the time development of the melting front at a specified location x_k.

NONDIMENSIONALIZATION

Dimensionless variables are defined as follows:

$$\theta = (T_i - T_f)/(T_w - T_f), \quad \zeta = x/H$$

$$A = H/L, \quad \delta = \delta/L, \quad \tau = Ste\, Fo$$

$$Ste = c_p(T_w - T_f)/\Delta h_f, \quad Fo = \alpha t/L^2 \tag{13}$$

where A is the aspect ratio, Ste the Stefan number and Fo the Fourier number. Hence, at the kth step, the non-dimensional core temperature is given by

$$\left\{\frac{\theta_k}{1-\theta_k}\right\}^{4n/3} = \frac{\displaystyle\int_0^{\zeta_k} (1-\theta)^{1/3-4n/3}\,\mathrm{d}\zeta}{\displaystyle\int_{\zeta_k}^{1} \cos^{-2/3}\phi\, \theta^{1/3-4n/3}\,\mathrm{d}\zeta} \tag{14}$$

and the non-dimensional melt layer advancement rate is

$$\mathrm{d}\delta_k/\mathrm{d}\tau = Nu_k\, \theta_k. \tag{15}$$

The kth step Nusselt number is given by equation (1) as

$$Nu_k = C\, Ra_k^{1/4}\, F_k \tag{16}$$

where F_k is nondimensionalized as

$$F_k = \left\{\frac{\cos^{4/3}\phi_k\, \theta_k^{1/3-4n/3}}{A\displaystyle\int_{\zeta_k}^{1} \cos^{-2/3}\phi\, \theta^{1/3-4n/3}\,\mathrm{d}\zeta}\right\}^{1/4}. \tag{17}$$

The melted fraction, λ, is simply evaluated as

$$\lambda = \int_0^1 \delta \,\mathrm{d}\zeta. \tag{18}$$

During the initial conduction regime, the melting front is vertical, and is given by the quasi-steady solution of ref. [12]

$$\mathrm{d}\delta_k/\mathrm{d}\tau = 1/\delta_k \tag{19}$$

which yields a closed form solution

$$\delta_k = \sqrt{(2\tau)} \tag{20}$$

for all k.

DURATION OF THE CONDUCTION REGIME

The duration of the conduction regime, τ_c, is estimated by equating the relevant laminar Nusselt number and the conduction regime Nusselt number. For Prandtl numbers between 3 and 200, ref. [10] recommends the following correlation in the boundary layer regime [13]:

$$Nu_\delta = 0.36 Pr^{0.051}\, (\delta/H)^{0.36}\, Ra_\delta^{0.25} \tag{21}$$

where both Nu_δ and Ra_δ are based on δ and $(T_w - T_f)$ as the characteristic length and temperature difference, respectively. Equation (21) has been tested for $Ra(H/\delta)^3 < 4 \times 10^{12}$. For the conduction regime

$$Nu_\delta = 1.0. \tag{22}$$

Equating equations (21) and (22), the melt layer thickness corresponding to the end of the conduction regime can be solved as

$$\delta_c = \left\{\frac{A^{0.36}}{0.36 Pr^{0.051}\, Ra_L^{0.25}}\right\}^{1/1.11}. \tag{23}$$

Hence the duration of the conduction regime is given by

$$\tau_c = \bar{\delta}_c^2/2. \quad (24)$$

A similar procedure has been used in refs. [2, 14].

NUMERICAL PROCEDURE

$0 < \tau < \tau_c$ *Conduction regime*

The time development of the melting front is given by equation (19).

$\tau > \tau_c$ *Laminar convection regime*

The melt layer thickness distribution at time $\tau > \tau_c$ is denoted as $\bar{\delta}_k^n$, $k = 1, 2, \ldots, N$, where N is the total number of nodes. The angle of inclination, ϕ_k^n, is expressed as

$$\phi_k^n = \tan^{-1}\{(\bar{\delta}_{k+1}^n - \bar{\delta}_k^n)/\Delta\zeta\}. \quad (25)$$

The temperature distribution, θ_k^n, can now be found from equation (14). The Nusselt number Nu_k^n is found from equation (16). Finally, the new melt layer thickness distribution at time $\tau + \Delta\tau$ is approximated by the following explicit equation:

$$\bar{\delta}_k^{n+1} = Nu_k^n \theta_k^n \Delta\tau + \bar{\delta}_k^n. \quad (26)$$

The whole calculation cycle can then be repeated.

As the melting front advances, $\bar{\delta}_k$ approaches the value of unity (i.e. the physical cold wall). Once $\bar{\delta}_k$ takes on the value of unity or slightly higher than unity, it is set to unity for the remaining computation. The corresponding angle ϕ_k is set to zero. The time step, $\Delta\tau$, is chosen such that $\bar{\delta}_k$ will not exceed unity too much during the advancement calculation.

Initially, the Nusselt number at node N is infinite. Hence, equation (26) is undefined at $k = N$. At present, the value of $\bar{\delta}_N$ is obtained by extrapolation. Once $\bar{\delta}_N$ reaches one, the remaining computation can proceed as usual without any singularity node. This procedure is rather crude and is partly responsible for the large discrepancy at the top portion of the melting front prediction, as will be discussed later. As a final note, all integrals are evaluated by the simple trapezoidal rule.

RESULTS AND DISCUSSIONS

A sensitivity study of the time step, $\Delta\tau$, and the mesh size, $\Delta\zeta$, was carried out. Figure 4 shows the melting front development for two time steps and two mesh sizes. For each mesh size, the numerical results are practically identical for the two time steps used. However, the shapes differ for the two mesh sizes, especially in the top portion and before the melting front reaches the cold wall. This is due to the previously mentioned extrapolation treatment of the singularity node, N. The melted fraction over the range of $\Delta\tau$ and $\Delta\zeta$ shown in Fig. 4 was found to be almost the same as expected from the low sensitivity of the melting front position on $\Delta\tau$ and $\Delta\zeta$ depicted in the same figure.

Comparisons are now made with existing experimental and numerical data, for a liquid having a Prandtl number of 50 [2–4]. The corresponding value for n is 3.0 [11]. Based on the sensitivity study, all comparisons are made with a mesh size of 0.1 and a time step of 0.004.

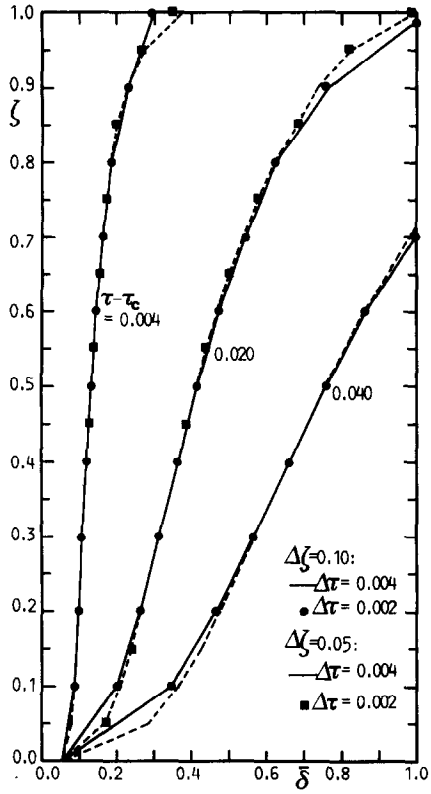

FIG. 4. Sensitivity of melting front on $\Delta\tau$ and $\Delta\zeta$.

Consider the melted fraction, λ, first. Figure 5 shows the variation of λ with a non-dimensional time based on the height of the enclosure. Comparison is made with the experimental data from ref. [4], based on an aspect ratio of 2. The agreement is good. Comparisons with the numerical results from ref. [3] for three different aspect ratios are shown in Fig. 6. Good agreement is obtained for the 1.13 aspect ratio case. As the aspect ratio increases, the melting rate increases, and the comparison becomes worse. This may be attributed to the inadequacy of the quasi-steady assumption (which is also used in ref. [3]) in high melting rate cases. Finally, comparison with the experimental data of ref. [2] in physical time is shown in Fig. 7. Good agreement is also obtained.

Next consider the development of the melting front. Figure 8 compares the present results with the measurements from ref. [2]. Results are comparable in the central portion of the melting front. However, large discrepancy exists at the top and bottom region. At the top, the large error is partly due to the extrapolation treatment of the Nth node, and partly to the one-dimensional approximation of the melting front, which neglects the curvature of the interface, as men-

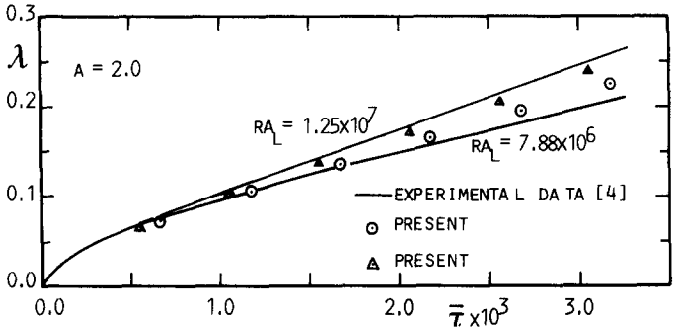

FIG. 5. Comparison of melting rate with ref. [4].

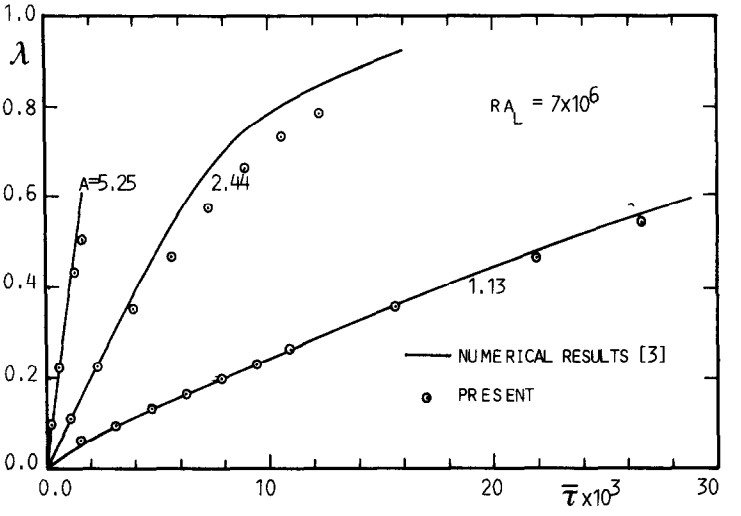

FIG. 6. Comparison of melting rate with ref. [3].

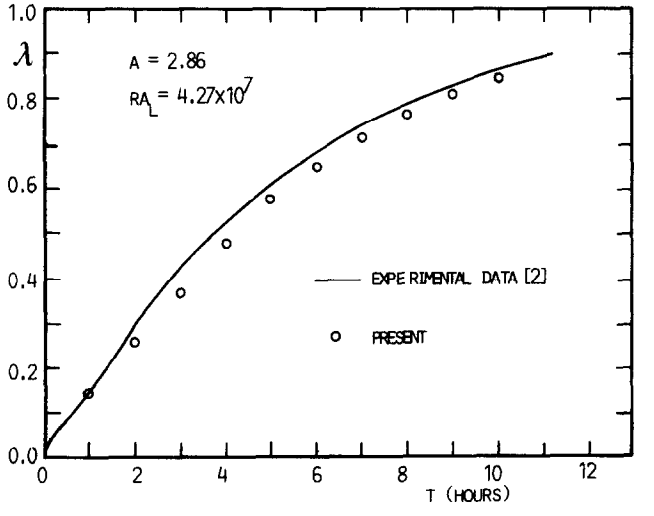

FIG. 7. Comparison of melting rate with ref. [2].

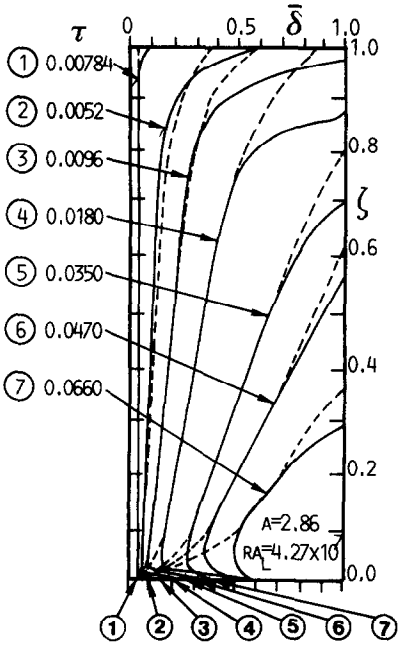

FIG. 8. Comparison of melting front with ref. [2].

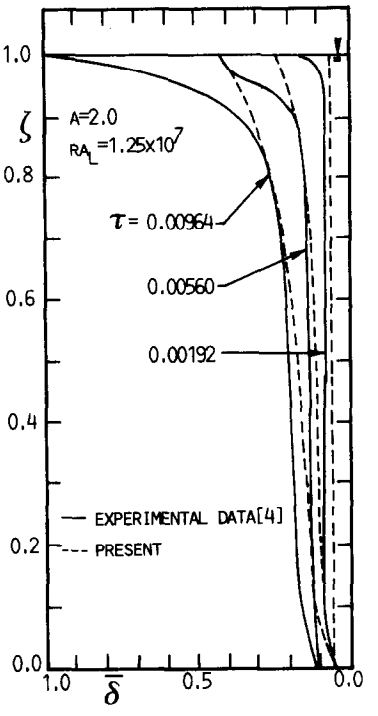

FIG. 9. Comparison of melting front with ref. [4].

tioned before. Since the melting front is highly curved at the top, the step approximation (refer to the numerical procedure) is seriously in error. At the bottom, the melting front location remains at the conduction regime value, δ_c (see equation (23)). This is an inherent drawback of the present model. As the model switches from the conduction regime to the convection regime, the local heat flux at the bottom vanishes because the temperature difference there is zero. Hence, from equation (15), δ_1 remains at the conduction value δ_c in the convection regime. In reality, one still expects some heat transfer to the melting front at the bottom in the convection regime. If one assumes the local quasi-steady conduction solution applies at the bottom, the time development of δ_1 will be given by equation (19) in the convection regime. The corresponding locations of δ_1 are indicated by arrows below Fig. 8. In addition, the inadequacy of the CLAM model in the recirculating zones near the top and bottom part of the enclosure also contributes to the larger discrepancies between prediction and experimental data in these regions.

Exact comparison with experimental data at the bottom is difficult due to the individual experimental setup. In the present case, prediction based on pure conduction, i.e. equation (19), underpredicts the bottom melting front location. However, the opposite has been found for the case of melting of a pure metal [15]. In addition, an experimental study of melting around a vertical cylinder has indicated that the melting front is stationary at the bottom in the convection regime [14].

Finally, the present model is compared with the experimental melting front data of ref. [4] in Fig. 9. The above comments apply to this case as well. However, comparison in the central part of the melting front is not as good as that shown in Fig. 8. The exact cause for this poorer agreement is not known.

CONCLUSIONS

In summary, an engineering analysis of the heat transfer process during melting of a PCM in a vertical rectangular enclosure has been proposed. The model is based on the general concepts of CLAM. The local heat transfer coefficient at the melting front is determined from a typical existing Nusselt number correlation valid for laminar boundary layer flow over a surface. Comparisons with existing numerical results and experimental data indicate that the present analysis gives adequate prediction of the melting rate and the movement of the melting front. This is notwithstanding the various simplifying, sometimes drastic, assumptions made during the model development. The present model requires minimal programming effort and insignificant computational times. In view of the fact that most existing front tracking numerical schemes still need prohibitable amounts of CPU times on mainframes, it is hoped that the present analysis can be a practical engineering tool for studying phase change systems, where detailed information on the velocity and temperature field is not needed.

Acknowledgements—The author wishes to thank Dr L.-J. Fang for providing the opportunity to carry out this study during his sabbatical leave at the Industrial Technology Research Institute, Hsinchu, Taiwan, R.O.C. Thanks are

also due to the reviewers for their critical comments and suggestions which have been incorporated in this final version.

REFERENCES

1. B. W. Webb and R. Viskanta, Analysis of heat transfer during melting of a pure metal from an isothermal vertical wall, *Numer. Heat Transfer* **9**, 539–558 (1986).
2. C. Benard, D. Gobin and F. Martinez, Melting in rectangular enclosures: experiments and numerical simulations, *Trans. ASME J. Heat Transfer* **107**, 794–803 (Nov. 1985).
3. A. Gadgil and D. Gobin, Analysis of two-dimensional melting in rectangular enclosures in presence of convection, *Trans. ASME J. Heat Transfer* **106**, 20–26 (Feb. 1984).
4. C.-J. Ho and R. Viskanta, Heat transfer during melting from an isothermal vertical wall, *Trans. ASME J. Heat Transfer* **106**, 12–19 (Feb. 1984).
5. C. A. Brebbia, J. C. F. Telles and L. C. Wrobel, *Boundary Element Techniques*. Springer, New York (1984).
6. B. W. Webb and R. Viskanta, Natural-convection-dominated melting heat transfer in an inclined rectangular enclosure, *Int. J. Heat Mass Transfer* **29**, 183–192 (1986).
7. M. H. Chun, H. O. Choi, H. G. Jun and Y. S. Kim, Phase-change front prediction by measuring the wall temperature on which solidification occurs, *Int. J. Heat Mass Transfer* **30**, 2614–2650 (1987).
8. V. R. Voller, M. Cross and N. C. Markatos, An enthalpy method for convection/diffusion phase change, *Int. J. Numer. Meth. Engng* **24**, 271–284 (1987).
9. V. R. Voller and C. Prakash, A fixed grid numerical modelling methodology for convection–diffusion mushy region phase-change problems, *Int. J. Heat Mass Transfer* **30**, 1709–1719 (1987).
10. G. D. Raithby and K. G. T. Hollands, Natural convection. In *Handbook of Heat Transfer Fundamentals* (Edited by W. M. Rohsenow, J. P. Hartnett and E. N. Ganic), 2nd Edn, Chap. 6. McGraw-Hill, New York (1985).
11. G. D. Raithby, K. G. T. Hollands and T. E. Unny, Analysis of heat transfer by natural convection across vertical fluid layers, *Trans. ASME J. Heat Transfer* **99**, 287–293 (May 1977).
12. H. S. Carslaw and J. C. Jaegar, *Conduction of Heat in Solids*, 2nd Edn, Chap. 11. Oxford University Press, Oxford (1959).
13. N. Seki, S. Fukusako and H. Inaba, Heat transfer of natural convection in a rectangular cavity with vertical walls of different temperatures, *Bull. J.S.M.E.* **21**, 246–253 (1978).
14. P. R. Souza Mendes and A. C. Pinho Brasil, Jr., Heat transfer during melting around an isothermal vertical cylinder, *Trans. ASME J. Heat Transfer* **109**, 961–964 (Nov. 1987).
15. C. Gau and R. Viskanta, Melting and solidification of a pure metal on a vertical wall, *Trans. ASME J. Heat Transfer* **108**, 174–181 (Feb. 1986).

ANALYSE INDUSTRIELLE DU TRANSFERT THERMIQUE PENDANT LA FUSION DANS DES CAVITES RECTANGULAIRES VERTICALES

Résumé—On présente une méthode simple d'analyse industrielle pour le mécanisme du transfert de chaleur pendant la fusion dans une cavité rectangulaire verticale. L'analyse est basée sur la méthode approchée de la couche de conduction (CLAM) précédemment appliquée à l'étude de la convection naturelle sans changement de phase dans des cavités. Semblable à de nombreux schémas numériques existants, le modèle actuel met en évidence le front de fusion pendant le mécanisme de fusion. Néanmoins, il n'est pas nécessaire de connaitre en détail les champs de vitesse et de température. Les résultats numériques sont obtenus avec une relative facilité et des temps de calcul insignifiants. On fait une comparaison avec les études numériques existantes et les données expérimentales pour le temps de développement du front de fusion et la fraction fondue. On obtient un bon accord.

UNTERSUCHUNG DER WÄRMEÜBERTRAGUNG BEIM SCHMELZVORGANG IN EINEM VERTIKALEN RECHTECKIGEN HOHLRAUM

Zusammenfassung—Diese Abhandlung zeigt eine einfache, anwendungsorientierte Analysemethode für die Wärmeübertragung beim Schmelzvorgang in einem vertikalen, rechteckigen Hohlraum. Das Verfahren basiert auf der CLAM-Methode, die ursprünglich zur Untersuchung von natürlicher Konvektion ohne Phasenwechsel in Hohlräumen angewendet wurde. Ähnlich wie bei den meisten bestehenden numerischen Verfahren wird der Verlauf der Schmelzfront während des Schmelzvorgangs dargestellt. Detaillierte Geschwindigkeits- und Temperaturfelder werden dabei jedoch nicht benötigt. Die Ergebnisse werden relativ einfach bei unwesentlichem Rechenaufwand gewonnen. Ein Vergleich mit bestehenden numerischen Untersuchungen und experimentell ermittelten Werten über das Fortschreiten der Schmelzfront und des Schmelzanteils zeigten gute Übereinstimmung.

ТЕОРЕТИЧЕСКИЙ АНАЛИЗ ТЕПЛОПЕРЕНОСА ПРИ ПЛАВЛЕНИИ В ВЕРТИКАЛЬНЫХ ПРЯМОУГОЛЬНЫХ ПОЛОСТЯХ

Аннотация—Предложен простой инженерный метод анализа теплопереноса при плавлении в вертикальной прямоугольной полости. Анализ основан на приближении пограничного слоя, ранее применявшемся при изучении естественной конвекции без фазовых превращений в камерах. Подобно большинству известных численных схем, данная модель позволяет следить за фронтом плавления, причем без необходимости точного определения полей скорости и температуры. Численые результаты получаются относительно просто, не требуя больших затрат машинного времени. Проведено сравнение полученных результатов с известными численными и экспериментальными данными по движению фронта плавления и зависимости доли расплава от времени, давшее хорошее совпадение.